

Neural network-based Load Balancing and Reactive Power Control by Static VAR Compensator

Ismail K. Said and Marouf Pirouti

Abstract— unbalanced loads in three phase systems produce undesired negative and zero sequence currents. Negative sequence currents will cause excessive heating of electrical machines, saturation of transformers, ripple in rectifiers or even instability problems of generators. Zero sequence currents cause not only excessive power losses in neutral lines but also protection and interference problems. To achieve a balanced operation for unbalanced AC system and improve power transfer capability, reactive compensation is used. This study use Artificial Neural Network (ANN) deals with an active scheme aiming to attenuate the negative sequence component of the line currents associated with an unbalanced three phase load. The system also assures a unity power factor at the load bus. The proposed structure uses a Y-connected capacitor bank and Δ -connected thyristor reactor which is controlled by ANN, So that, the amount of reactive power is being controlled. Three different networks are learned by both real and imaginary part for three phase load currents (I_x , I_y , I_z). Hundreds of unbalanced cases in a 33 (KV) system are simulated for this purpose. Study show that ANN-based reactive power compensation is completely suitable for an on-line load balancing and reactive power compensation in the system by measuring both real and imaginary part of three phase load currents and processing them by ANN.

Index Terms— ANN, Load balancing, Static VAR compensation

I. INTRODUCTION

Reactive power requirements of industrial loads such as electric arc furnaces, rolling mills, traction loads, arc welders, etc. are often unbalanced and could vary in a wide range within short period of time. These loads lead to unbalanced system voltages and fluctuations in the supply voltage causing many undesirable effects such as malfunction of protective relays and sensitive loads, incandescent lam flicker, and television picture distortion. Generally, the heavy loads which create these problems are located in industrial plants and supplied from on terminal network. Therefore they can be effectively compensated by shunt compensator connected at supply point of the industrial facility [1]

The recent tendency of load compensation theory is the transformation of an arbitrary ungrounded unbalanced linear load into a balanced three-phase load without changing the

real power exchange between loads and source, but by appropriate modification of reactive load power in each phase. Load compensation involves two separable acts; load balancing and Power factor correction. Both of them can be carried out together or separately. Modification of the reactive power of the phases can be done by connecting variable reactive source in the shunt with load element.

Despite the emergence of modern device such as STATCOMs, Static VAR Compensator (SVSc) are still popularly used in modern power distribution systems for load balancing and power factor correction due its lower cost [2].

A Static VAR Compensator generally consists of a Thyristor Controlled Reactor (TCR) and a Thyristor Switched Capacitor (TSC) and compensates loads through generation or absorption of reactive power. The operation of thyristor-controlled reactors at appropriate conduction angles can be advantageously used to meet the unbalanced and varying reactive power demand in a system [1-5].

In this study Thyristor Controlled Reactor -Fixed Capacitor (TCR-FC) is used and ANN capability in pattern recognition is applied to control of reactive power by controlling of firing angle of thyristors. Appropriate firing angles for each pair of thyristors ($\alpha T1$, $\alpha T2$, $\alpha T3$) are predicted by three different ANNs for any unbalanced condition in the system.

II. STATIC VAR COMPENSATOR (TCR-FC TYPE)

The term static VAR system has been adopted to apply to a number of static VAR compensation devices for use in shunt reactive control. These devices consist of shunt connected, static reactive elements (linear or nonlinear reactor and capacitor) configured into a VAR compensating system, and their distinction is that the shunt reactive power flowing in these devices is controllable over some rated range of VARs. The basic system consists of parallel combination of fixed capacitors and thyristor switch by an angle α , in each half cycle (α increased from 90o to 180o) the technique of controlling the conduction intervals of the thyristor switch, generate harmonic current components [6]. Fast response and the capability of balance load make the fixed capacitor, thyristor controlled inductor particularly advantageous for compensating those loads which present rapidly at various unbalanced conditions. In this study capability of ANN is used to recognize unbalance conditions and to provide proper firing angle as quickly as possible for thyristors which provide reactive power to balance the system. FC-TCR is

Ismail K. Said is with the Electrical Department of Salahaddin University, Erbil, Iraq.

Marouf Pirouti is with the Electrical Department of Salahaddin university, Erbil, Kurdistan region, Iraq. Email: m.pirouti@gmail.com. Tel:00964-7504716749

shown in Fig.1.

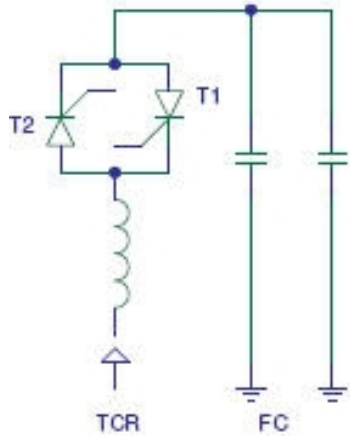


Fig.1 Fixed capacitor, thyristor-controlled inductor type

III. ARTIFICIAL NEURAL NETWORKS

Artificial neural networks have been widely used in the power industry in fault classification, protection, fault diagnosis, relaying schemes, load forecasting and power generation. At present most ANNs are built upon the environment of real numbers.

However it is well known that in computations related to electric power systems, such as load flow analysis and fault level estimation, complex numbers are extensively involved. The reactive power drawn from a substation, the impedance, bus bar voltages and currents are all expressed in complex numbers. But ANNs are able to deal with complex numbers by treating the real parts and imaginary parts independently. ANNs have been proved to be capable of learning from raw data. They can be used to identify relations within raw data not explicitly given or even known by human experts and there is no need to assume any linear relationship between data. ANNs represent the promising new generation of information processing networks [7].

ANNs can supplement the enormous processing power of the digital computer with the ability to make sensible decision and to learn by ordinary experience. ANNs have widely been used in electric power engineering. For energy management, load flow and optimum power flow problems are solved by ANNs to estimate bus bar voltages. ANNs can perform the task of associative memory. Since information is stored in the connections and it is distributed throughout, the network can function as a memory. This memory can work even in the presence of certain level of internal noise. ANNs are somewhat fault tolerant in the sense that information is not lost even if some connections are snapped or some units are not functioning. It can deal with data that are not only noisy, but also fuzzy, inconsistent due to associative and distributed nature. They have ability to approximate functions and automatic similarity based generalization. ANNs are distinguished based on the signal flow direction and is classified into, feed forward network and feed back network. A feed forward network is a network in which signal propagate in only one direction from an input stage through intermediate neurons to an output stage. It has no memory since output solely depends on the input. A feed back

network is a network in which signal propagate from the output of any neuron to the input of any neuron. What is fed back is usually the error in the output modified appropriately according to the requirement needed. Both these models will have the three or subgroups of processing elements via, input layer, hidden layer, and output layer.

In this study multi layer feed forward network with ML back propagation training algorithm is used [8].

IV. MATHEMATICS MODELING AND SIMULATION

In this study a three-phase 33 KV system as shown in Fig.2, is considered. The substation is assumed to be a constant balanced voltage source and the three distribution line impedances are equal. The unbalance of the single phase loads in the system will cause an asymmetry of the line currents, and consequently unequal voltage drops on the line distribution lines. In these conditions the load bus voltages will become unbalanced. In order to improve the load power factor and to balance the line currents a fast action system is connected to the load bus. It consists of a star connected capacitor bank (Y-CCB) and a delta connected TCR bank (Δ -TCR). The thyristors in the TCR are driven to provide the necessary amount of reactive power to each phase. From Fig.2, we have

- I_{12}, I_{23}, I_{31} the complex values of the fundamental currents in the TCR branches.
- I_{as}, I_{bs}, I_{cs} the complex values of the line currents (supply currents)
- I_{1c}, I_{2c}, I_{3c} the complex values of the currents in the capacitors.
- I_x, I_y, I_z the complex values of the unbalanced load currents.

The load currents are:

$$\left. \begin{aligned} I_x &= I_{xl} \\ I_y &= h^2 * I_{yl} \\ I_z &= h * I_{zl} \end{aligned} \right\} \text{---- (1)}$$

The currents through the Y-CCB branches are balanced, which consists only reactive component and for phase (a) can be expressed as

$$I_c = V_a / X_c \text{---- (2)}$$

The values of the currents that must flow in the Δ -TCR branches, in order to obtain the desired effects are:

$$\left. \begin{aligned} I_{12} &= \frac{1}{\sqrt{3}} [I_c + \text{imag}(I_{xl}) + \text{imag}(I_{yl}) - \text{imag}(I_{zl})] \\ I_{23} &= \frac{1}{\sqrt{3}} [I_c - \text{imag}(I_{xl}) + \text{imag}(I_{yl}) + \text{imag}(I_{zl})] \\ I_{31} &= \frac{1}{\sqrt{3}} [I_c + \text{imag}(I_{xl}) - \text{imag}(I_{yl}) + \text{imag}(I_{zl})] \end{aligned} \right\} \text{---- (3)}$$

The instantaneous value of the current through one leg of the Δ -TCR bank is the sum of forced and natural responses [9]:

$$i = \sqrt{2} \frac{V}{w * L} \left[\sin(wt - \frac{p}{2}) - \sin(a - \frac{p}{2}) \right] \text{--- (4)}$$

Where $\frac{p}{2} < a < p$

In order to calculate the values of the firing angle, we must calculate the ratio of I_{RMS}/I_{RMS}^* Table.1, where I_{RMS} represents the required RMS value of the current through TCR and I_{RMS}^* is the maximum value of the TCR's current ($\alpha=\pi/2$)

TABLE I

I_{RMS}/I_{RMS}^* s	a (RAD)	I_{RMS}/I_{RMS}^* s	a (RAD)
0	3.14	0.55	1.956
0.1	2.708	0.6	1.909
0.15	2.567	0.65	1.863
0.2	2.376	0.7	1.818
0.25	2.3	0.75	1.775
0.3	2.232	0.8	1.733
0.35	2.17	0.85	1.691
0.4	2.112	0.9	1.65
0.45	2.058	0.95	1.61
0.5	2.006	0.99	1.579

Since the currents in the bank are in quadrate lagging the line voltages, they have the expressions:

$$\left. \begin{aligned} I_{12} &= -h * I_{12} \\ I_{23} &= -I_{23} \\ I_{31} &= -h^2 * I_{31} \end{aligned} \right\} \text{--- (5)}$$

Using first Kerchief's law, the supply currents will be:

$$\left. \begin{aligned} I_{as} &= I_c + I_{12} - I_{31} + I_x \\ I_{bs} &= h^2 * I_c + I_{23} - I_{12} + I_y \\ I_{cs} &= h * I_c + I_{31} - I_{23} + I_z \end{aligned} \right\} \text{--- (6)}$$

In this paper, based above relations the value of firing angle of TCR' Thyristors (one branch) as function of I_{RMS} is calculated. In order to generalize, these values are calculated as a function of I_{RMS}/I_{RMS}^* ratio Table.1, where I_{RMS} represents the required RMS value of the current through TCR and I_{RMS}^* is the maximum value of the TCR's RMS current at ($\alpha=\pi/2$). For providing data in ANN application, based above mathematical background a program in MATLAB is written for this purpose [10]. Hundreds of unbalanced conditions by using this program are simulated and appropriate α is obtained.

V. RESULT

Multilayer feed forward networks were chosen to process the prepared input data. In this study 749 unbalanced cases were simulated and appropriated firing angle for each pair of thyristors ($T1, T2, T3$) was obtained. 66 percent of all data was used for training and others were applied for testing the networks. Three multilayer feed forward networks with proposed scheme as shown in Fig.2. are considered for this propose. Both real and Img parts of three phase load current I_x, I_y and I_z after normalization were fed to neural networks. The networks' architectures were decided empirically by

using trail and error method for choosing best ANN structure which is involved to training and testing different number of networks. Unfortunately, it is difficult to know beforehand how large a network should be for a specific application. If a larger network is used the more complex functions of the network can be created and if small enough networks are selected, they will not have enough power to over fit the data. Various networks with different number of neurons in their hidden layers were trained with ML algorithms. Ultimately, three networks with **Logsig-Logsig-purelin activation function and 6-7-6-1 neuron in input-first hidden layer-second hidden layer-output** were suitable for this application by which the mean square errors for all testing data for all three networks were 0.025.

A. Reactive power compensation

Testing result for each network for 60 unbalanced conditions is shown in Table.2. For each unbalanced condition both real and imag parts of three phase current as mentioned before were used. And at the right side of the table both desired and actual firing angle for compensate reactive power during load fluctuation is come. The amount of reactive power which is supplied by the system (Qs) with out compensation and with compensation (ANN-based FC-TCR) for all 60 cases in Table.2, are shown in Fig.3.

B. Balancing three phase currents

The three phase currents which are supplied by the system (I_{as}, I_{bs} and I_{cs}) also balanced by this purposed scheme. The amount of three phase currents for all 60 cases in Table.2 after power reactive compensation and balancing system are shown in Fig.4. Also unbalanced factor for all 60 cases before and after compensation is shown in Table.3.

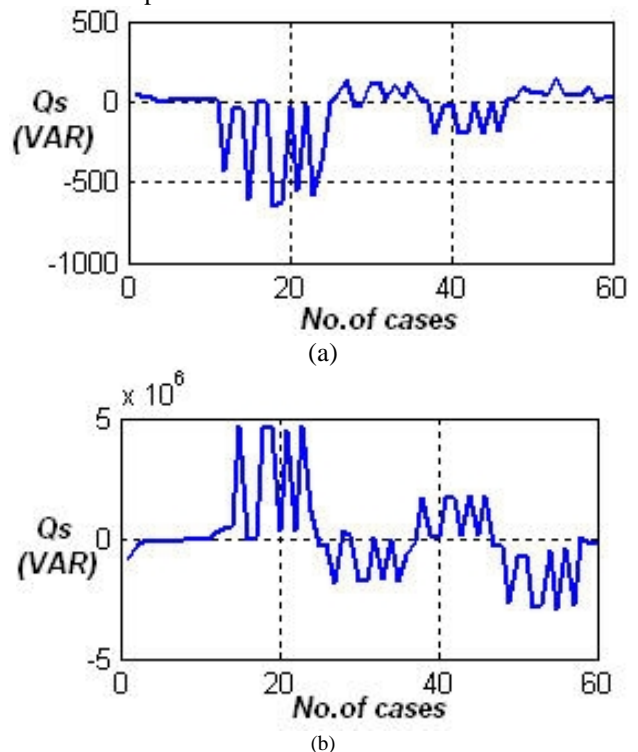


Fig. 2 (a) Qs Supplied by the system with out compensation (b) Qs Supplied by the system with ANN based FC-TCR compensation

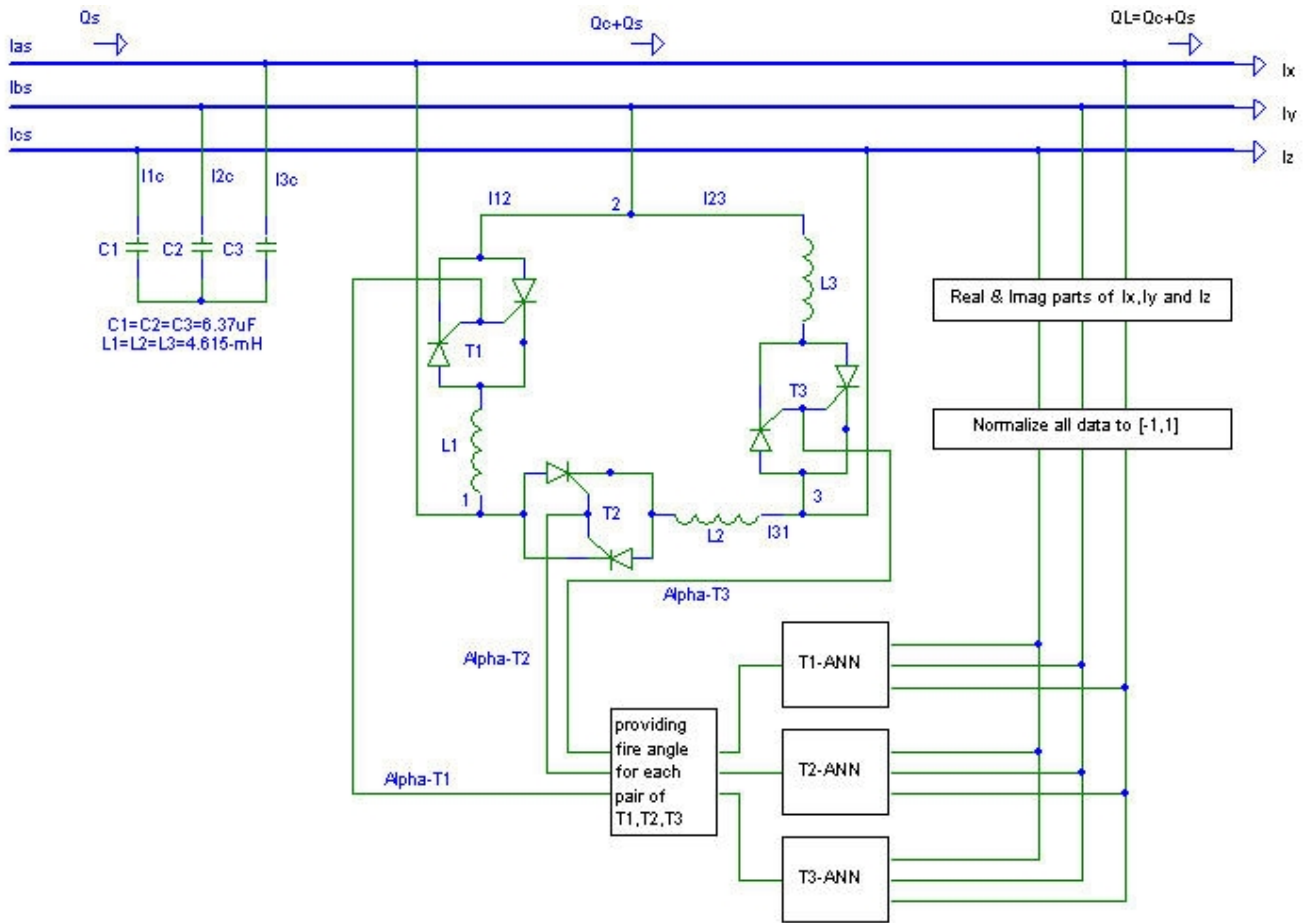


Fig. 3 Load compensator modeling using (TCR) &FC combined with ANN

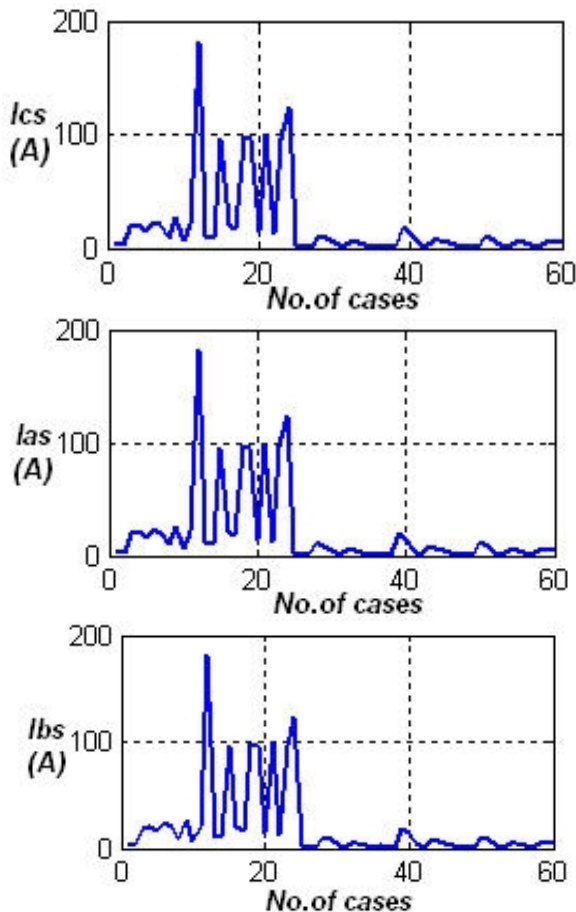


Fig. 4 Three phase current after power reactive compensation by ANN based FC-TCR for all 60 cases in Table .2

I. CONCLUSION

A medium voltage system 33KV is selected for this study and ANN based FC-TCR compensator is considered. ANN capabilities in pattern recognition and classification are designed. Simulation studies are performed and module's performance with different system conditions is investigated. It was found that ANN application is very accurate and useful for control of reactive power and balancing system.

- From the study Table.2. It can be seen that ANN is very quick and reliable to find appropriate firing angle for thyristors which are concerning to compensate any unbalanced condition in the system.
- Control of reactive and minimizing the reactive power drawn from the supply. Fig.3. (a) and (b), shows by selecting appropriate firing angle for Thyristors amount of reactive power drawn from the supply is minimized significantly so that power factor also is corrected.

Balancing three phase currents and minimizing the unbalanced factor, from the Table.3. and Fig.4. It can be observed that this proposed algorithm is able to balance three phase current and minimize the unbalanced factor ($I_{Negative-sequence}/I_{positive-sequence}$) in any unbalanced condition.

TABLE II: DESIRED AND ACTUAL FIRING ANGLE OF T1, T2 AND T3 FOR ANN-BASED FC-TCR TO COMPENSATE REACTIVE POWER AND BALANCE SEVERAL UNBALANCED CONDITIONS

Real (I_a)	Im (I_a)	Real (I_b)	Im (I_b)	Real (I_c)	Im (I_c)	Desired fire angle (Angle)			ANN fire angle (Angle)		
						α_{T1}	α_{T2}	α_{T3}	α_{T1}	α_{T2}	α_{T3}
9.4792	46.36	-10.65	28.28	15.074	19.888	158.05	148.88	179.29	158.1	148.88	176.76
2.2872	15.761	-2.3191	8.0488	6.6639	7.9163	156.88	147.66	156.79	156.87	147.66	156.8
0.86958	6.7846	26.281	-12.385	30.176	19.206	132.12	147.53	178.69	132.09	147.53	176.71
28.259	1.7528	16.7	7.2926	17.683	-5.4883	156.42	147.54	139.33	156.42	147.54	139.32
19.916	11.255	10.989	10.666	15.963	3.2289	157.58	149.5	150.36	157.57	149.5	150.36
7.4994	10.721	29.168	-7.3665	33.998	20.442	135.66	149.29	178.03	135.64	149.29	176.25
2.2415	6.0672	27.478	-12.103	30.596	18.837	132.09	148.01	175.32	132.07	148.01	175.64
11.391	0.28394	8.5054	1.7631	8.6675	-1.4758	150.15	147.5	145.22	150.15	147.5	145.23
10.466	2.5268	33.441	-12.228	34.731	15.045	132.14	147.72	160.85	132.12	147.72	160.84
7.1755	4.7604	5.6047	3.2983	7.6567	2.6689	151.48	148.42	150.59	151.48	148.42	150.59
3.2673	4.4171	28.949	-12.682	30.916	18.108	131.54	148.27	169.53	131.52	148.27	169.57
154.67	100.17	199.48	83.457	191.56	130.61	158.32	128.33	120.15	158.08	128.09	120.41
4.6025	11.449	21.186	16.628	8.4097	28.399	147.25	165.78	158.32	147.25	165.81	158.31
10.765	-1.8206	16.293	11.315	2.1542	9.5336	147.47	158.23	144.72	147.47	158.23	144.73
141.34	-79.761	143.71	83.846	0.84437	4.0854	147.5	115.05	101.43	147.49	115.04	101.53
27.883	1.0196	17.194	6.6876	17.631	-5.4041	155.87	147.7	139.3	155.87	147.7	139.3
19.474	3.889	17.366	7.5233	15.273	3.8792	152.9	152.89	147.69	152.9	152.89	147.69
142.19	-75.834	145.29	83.014	6.1775	6.2751	148.19	115.62	102.68	148.19	115.62	102.86
141.87	-79.582	144.06	83.309	1.9045	3.752	147.48	115.28	101.5	147.48	115.27	101.6
19.901	-4.7815	15.44	7.6043	6.9447	-2.4522	151.4	154.32	136.93	151.4	154.32	136.92
147.23	-77.897	144.1	81.989	7.201	-0.6685	151.04	117.02	101.26	151.02	117.05	101.33
15.806	-3.5845	15.512	8.0305	5.6005	1.9675	149.38	156.06	140.27	149.38	156.06	140.27
142.67	-79.669	143.89	82.681	2.6827	2.5587	147.85	115.67	101.38	147.84	115.67	101.47
170.39	155.66	116.98	226.35	82.47	144.74	101.17	105.43	149.14	101.11	107.05	149.01
13.666	36.188	-6.612	38.307	1.6937	19.687	158.04	158.1	157.33	158.1	158.1	157.34
0.31108	18.859	-3.174	12.763	3.8483	12.794	157.6	152.36	157.61	157.6	152.36	157.61
-52.583	99.311	-1.4808	5.457	54.248	96.643	153.27	149.61	110.61	153.28	149.61	110.6
9.165	2.0098	16.747	7.3797	8.3059	11.261	146.06	157.09	151.82	146.06	157.09	151.82
9.2313	8.6421	11.207	11.589	7.6679	11.827	153.44	156.51	153.72	153.44	156.51	153.72
-46.794	99.319	2.9882	9.6432	55.759	97.597	155.07	153.14	111.22	155.08	153.13	111.13
-51.741	98.415	0.0679	5.2016	54.889	96.679	152.52	150.11	110.73	152.53	150.11	110.7
0.27945	6.342	6.7984	2.7669	6.6352	10.2	146.66	152.31	156.14	146.66	152.31	156.15
-48.868	93.189	6.0663	3.757	56.05	96.05	148.19	152.31	111.55	148.19	152.3	111.48
0.15865	9.6215	3.9692	4.7283	6.3017	10.475	150.41	151.61	156.71	150.41	151.61	156.72
-51.507	96.851	1.3654	3.9944	55.346	96.214	150.95	150.03	110.88	150.95	150.03	110.85
9.4792	46.36	-10.758	34.693	9.4661	23.002	157.46	155.06	168.15	157.45	155.05	167.84
2.2872	15.761	-2.427	14.462	1.0561	11.03	157.67	154.21	155.53	157.67	154.21	155.53
0.86958	6.7846	25.202	51.748	-25.902	50.338	153.31	134.62	151.47	153.31	134.63	151.46
28.259	1.7528	16.592	13.706	12.075	-2.375	157.39	154.12	137.23	157.38	154.12	137.22
19.916	11.255	10.881	17.079	10.356	6.3421	158.13	155.45	147.9	158.14	155.45	147.9
7.4994	10.721	28.089	56.766	-22.08	51.574	156.88	133.53	151.57	156.87	133.56	151.57
2.2415	6.0672	26.399	52.029	-25.482	49.969	153.27	134.31	150.5	153.27	134.33	150.5
11.391	0.28394	8.3975	8.1764	3.0597	1.6374	152.44	154.1	142.71	152.45	154.1	142.72
10.466	2.5268	32.362	51.905	-21.347	46.177	153.35	134.49	145.03	153.35	134.51	145.04
7.1755	4.7604	5.4968	9.7115	2.0489	5.782	153.61	154.75	148.14	153.62	154.75	148.14
3.2673	4.4171	27.871	51.45	-25.162	49.24	152.32	134.15	149.18	152.32	134.16	149.18
-1.4367	33.987	-1.3542	22.666	8.4097	28.399	159.82	157.21	173.45	159.8	157.2	173.75
4.7261	20.718	-6.2469	17.354	2.1542	9.5336	159.98	152.01	155.78	159.95	152.01	155.78
80.952	145.63	-81.687	144.24	0.84437	4.0854	92.55	149.54	151.54	92.535	149.54	151.53
21.844	23.558	-5.3457	12.727	17.631	-5.404	167.8	136.13	151.51	167.06	136.13	151.5
13.435	26.428	-5.1744	13.562	15.273	3.8792	172.19	140.73	157.12	172.8	140.73	157.12
81.793	149.55	-80.105	143.4	6.1775	6.2751	92.459	147.6	155.57	92.467	147.59	155.58
81.481	145.81	-81.336	143.7	1.9045	3.752	92.552	148.75	151.8	92.537	148.76	151.79
13.861	17.757	-7.0996	13.643	6.9447	-2.4522	166.33	142.48	148.77	166.2	142.48	148.77
86.833	147.49	-81.3	142.38	7.201	-0.6685	92.098	143.07	150.81	92.246	143.05	150.81
9.7668	18.954	-7.0281	14.069	5.6005	1.9675	162.03	145.25	152.46	162.05	145.25	152.46
82.273	145.72	-81.51	143.07	2.6827	2.5587	92.504	147.43	151.35	92.499	147.43	151.34
-1.0968	15.453	7.2799	12.416	5.7213	21.189	152.35	157.46	158.5	152.35	157.46	158.48
6.3654	11.579	2.0956	5.043	9.8917	4.6136	155.38	146.02	154.96	155.38	146.02	154.96
7.2547	6.1559	2.4033	3.9627	6.7287	0.85789	153.94	146.47	149.8	153.95	146.47	149.8

TABLE III: COMPARISON OF UNBALANCED FACTOR BEFORE AND AFTER COMPENSATION BY ANN-BASED FC-TCR FOR ALL 60 CASES IN TABLE 2

No.	ANN-based firing angle	Unbalanced Factor ($I_{\text{Negative-Sequence}}/I_{\text{Positive-sequence}}$)
-----	------------------------	---

of Cases	α_{T1}	α_{T2}	α_{T3}	Before compensation by ANN	After compensation by ANN
1	158.1	148.88	176.76	0.48349 + 0.082628i	-5.8841e-005 + 0.00020071i
2	156.87	147.66	156.8	0.47131 - 0.091306i	0.00033608 + 0.00023485i
3	132.09	147.53	176.71	-0.87715 - 0.32591i	0.00012208 + 2.8492e-005i
4	156.42	147.54	139.32	0.35379 - 0.0071042i	1.7023e-005 - 7.1541e-006i
5	157.57	149.5	150.36	0.28998 - 0.02824i	2.8042e-005 + 1.9746e-005i
6	135.64	149.29	176.25	-0.57638 - 0.31252i	8.5554e-005 + 1.0244e-005i
7	132.07	148.01	175.64	-0.83202 - 0.26615i	0.00010975 + 7.2112e-006i
8	150.15	147.5	145.23	0.19652 - 0.0059212i	8.7089e-005 + 3.0776e-005i
9	132.12	147.72	160.84	-0.59603 - 0.068953i	8.1494e-005 + 1.2133e-005i
10	151.48	148.42	150.59	0.11339 - 0.11441i	0.00012607 + 5.2621e-005i
11	131.52	148.27	169.57	-0.81648 - 0.1813i	0.00011268 + 1.4275e-005i
12	158.08	128.09	120.41	-0.12327 - 0.045872i	-1.0158e-005 - 4.1703e-005i
13	147.25	165.81	158.31	-0.44666 - 0.090579i	6.0334e-005 - 6.2883e-005i
14	147.47	158.23	144.73	-0.30924 + 0.63686i	4.4211e-005 - 7.3697e-005i
15	147.49	115.04	101.53	0.45808 + 0.87858i	-5.2027e-005 - 0.00011223i
16	155.87	147.7	139.3	0.33397 + 0.00018064i	1.6732e-005 - 7.6048e-006i
17	152.9	152.89	147.69	0.092713 + 0.096732i	2.7741e-005 + 2.0062e-006i
18	148.19	115.62	102.86	0.41417 + 0.83945i	-1.4359e-005 - 0.00011531i
19	147.48	115.27	101.6	0.45618 + 0.86723i	-4.7059e-005 - 0.00011392i
20	151.4	154.32	136.92	0.40884 + 0.35153i	4.105e-005 - 3.0514e-005i
21	151.02	117.05	101.33	0.4704 + 0.79962i	-2.3696e-005 - 9.7385e-005i
22	149.38	156.06	140.27	0.19769 + 0.49931i	4.2534e-005 - 2.6399e-005i
23	147.84	115.67	101.47	0.46333 + 0.85445i	-2.4928e-005 - 0.00010423i
24	101.11	107.05	149.01	0.050201 + 0.23306i	-7.1627e-005 - 5.3889e-005i
25	158.1	158.1	157.34	0.18296 + 0.3254i	-0.00023525 - 1.8856e-005i
26	157.6	152.36	157.61	0.27366 - 0.0072971i	0.0022917 + 0.0017958i
27	153.28	149.61	110.6	0.47855 - 0.7846i	0.06654 + 0.037667i
28	146.06	157.09	151.82	-0.33302 + 0.22627i	9.4001e-005 - 3.833e-005i
29	153.44	156.51	153.72	-0.11449 + 0.087503i	8.8795e-005 - 3.823e-005i
30	155.08	153.13	111.13	0.39851 - 0.76058i	0.00094954 + 0.00046875i
31	152.53	150.11	110.7	0.46127 - 0.79846i	0.0035897 + 0.0019921i
32	146.66	152.31	156.15	-0.32449 - 0.43634i	0.00025069 + 6.5928e-005i
33	148.19	152.3	111.48	0.38991 - 0.85506i	0.00087236 + 0.0004214i
34	150.41	151.61	156.72	-0.0048407 - 0.39894i	0.00029963 + 0.00012494i
35	150.95	150.03	110.85	0.45276 - 0.82253i	0.0021555 + 0.0012124i
36	157.45	155.05	167.84	0.34978 + 0.16706i	-7.5698e-005 + 0.00016962i
37	157.67	154.21	155.53	0.14935 + 0.14076i	0.0020669 + 0.00023622i
38	153.31	134.63	151.46	-0.813 + 0.023668i	-0.010024 - 0.057724i
39	157.38	154.12	137.22	0.43472 + 0.23734i	4.8329e-006 - 2.7463e-005i
40	158.14	155.45	147.9	0.25337 + 0.23557i	8.9823e-006 - 2.0795e-005i
41	156.87	133.56	151.57	-0.71211 + 0.1563i	-0.00015336 - 0.00078043i
42	153.27	134.33	150.5	-0.82988 + 0.057249i	-0.00033914 - 0.0033491i
43	152.45	154.1	142.72	0.26508 + 0.52177i	7.148e-005 - 1.1942e-005i
44	153.35	134.51	145.04	-0.86419 + 0.2831i	-9.9638e-005 - 0.00049174i
45	153.62	154.75	148.14	-0.033119 + 0.36008i	0.00011699 + 1.5952e-006i
46	152.32	134.16	149.18	-0.86905 + 0.085808i	-0.00017937 - 0.0015475i
47	159.8	157.2	173.75	0.19029 - 0.12934i	0.00035753 + 0.00012579i
48	159.95	152.01	155.78	0.30937 + 0.28038i	0.00080593 + 0.0016856i
49	92.535	149.54	151.53	0.48659 + 0.82558i	-0.22254 + 0.068836i
50	167.06	136.13	151.5	1.086 - 0.18335i	-7.8538e-006 + 7.3606e-005i
51	172.8	140.73	157.12	0.78615 - 0.039442i	4.6078e-005 + 0.00014608i
52	92.467	147.59	155.58	0.51992 + 0.78004i	-0.0023447 + 0.00022819i
53	92.537	148.76	151.79	0.49738 + 0.82302i	-0.011478 + 0.0037116i
54	166.2	142.48	148.77	1.0589 + 0.46163i	-1.8985e-006 + 0.00016308i
55	92.246	143.05	150.81	0.56664 + 0.83172i	-0.0018166 + 0.00021553i
56	162.05	145.25	152.46	0.72659 + 0.42584i	0.00012364 + 0.00026607i
57	92.499	147.43	151.34	0.51032 + 0.82925i	-0.0062414 + 0.0013709i
58	152.35	157.46	158.48	-0.12293 - 0.27993i	0.00026537 + 5.6398e-005i
59	155.38	146.02	154.96	0.38132 - 0.29454i	0.00013397 + 7.3042e-005i
60	153.95	146.47	149.8	0.43792 - 0.16386i	0.00014256 + 9.4868e-005i

REFERENCES

[1] D.Thukaram, A.Lomi and S.Chirattananon, Minimization of harmonics under three-phase unbalanced operation of static VAR compensators, Proceedings of the 12th International Conference on Power Quality (Power Quality '99), Chicago, USA, 1999.

[2] S.Y.Lee, C.J.Wu and W.N. Chang, A compact control algorithm for reactive power compensation and load balancing with static var compensator, Electric Power Systems Research, 58, 2001, pp.63-70.

[3] G.El-Saady, Adaptive static VAR controller for simultaneous elimination of voltage flicker and phase current imbalances due to arc furnace loads, Electric Power systems Research, 58, (2001) pp.133-140.

[4] G.Gueth, P.Enstedt, A Ray and R.W.Menzies, Individual phase control of static compensator for load compensation and voltage balancing and regulation, IEEE Trans, Power system, 2(4), 1987, pp.898-904

[5] A. Rajapakse and Anawat Puangpaioj, Harmonic reducing ANN controller for a SVS compensating unbalanced fluctuating loads, International Journal of Emerging Electric Power Systems, 7 (1), 2006, Article 5.

[6] R.Mohan Mathur and Rajiv K.Varma, Thyristor-based FACTS controllers for electrical transmission systems, John Wiley & sons publications, 2002 pp.63-71.

- [7] Jayabarathi.R.a and Devarajan.N.b, ANN based DSPIC controller for reactive power compensation, American journal of applied science, 4(7), 2007, pp.508-515
- [8] Hagan, M.T and M.Menhaj, Training feed forward networks with the Marquardt algorithm, IEEE. Transaction on Neural Networks, 5(6), 1999, pp.989-993
- [9] Muhammad H. Rashid, Power electronics circuits, devices and application, Second Edition, Prentice-Hall, 1993.
- [10] Brian D. Hahn and Daniel T. Valentine, Essential MATLAB for Engineers and Scientists, Third edition, Published by Elsevier, 2002.

Ismail K. Said, is graduated from Salahaddin University both BSc and MSc and now he is assistant lecturer at the Electrical Department, his area of interest is control of power system

Marouf Pirouti is graduated BSc from K.N.T University of Technology Tehran-Iran, 2003 and MSc from Salahaddin University, 2007. He is now assistant lecturer at Electrical Department of Salahaddin University and also he is teaching at the Dejeleh College .His area of interest is control of power and application of AI in power system.